NIH Public Access
Author Manuscript
Cell. Author manuscript; available in PMC 2012 October 28.

Published in final edited form as:
Cell. 2011 October 28; 147(3): 653–665. doi:10.1016/j.cell.2011.10.012.

Patterns of Spinal Sensory-Motor Connectivity Prescribed by a Dorsoventral Positional Template

Gülşen Sürmeli, **Turgay Akay**, **Gregory Ippolito**[1], **Philip W Tucker**[1], and **Thomas M Jessell**
Howard Hughes Medical Institute, Kavli Institute for Brain Science, Depts. of Neuroscience, and Biochemistry and Molecular Biophysics, Columbia University, New York, NY 10032

[1]Dept. of Cellular and Molecular Biology, The University of Texas at Austin, Austin, TX 78712

Summary

Sensory-motor circuits in the spinal cord are constructed with a fine specificity that coordinates motor behavior, but the mechanisms that direct sensory connections with their motor neuron partners remain unclear. The dorsoventral settling position of motor pools in the spinal cord is known to match the distal-to-proximal position of their muscle targets in the limb, but the significance of invariant motor neuron positioning is unknown. An analysis of sensory-motor connectivity patterns in FoxP1 mutant mice, where motor neuron position has been scrambled, shows that the final pattern of sensory-motor connections is initiated by the projection of sensory axons to discrete dorsoventral domains of the spinal cord without regard for motor neuron subtype, or indeed, the presence of motor neurons. By implication, the clustering and dorsoventral settling position of motor neuron pools serves as a determinant of the pattern of sensory input specificity, and thus motor coordination.

Introduction

The formation of synaptic connections is a defining moment in the assembly of neural circuits, providing a structural foundation for network activities that govern the subtleties of animal behavior. The intricate patterns of connectivity that characterize circuits in the mammalian central nervous system (CNS) depend on the diversification of neurons into distinct classes (Stevens, 1998), but the strategies and mechanisms used to translate neuronal subtype identity into selective connectivity remain unclear. Neuronal surface labels that serve as recognition cues for incoming axons have been proposed to underlie many stereotypic patterns of connectivity (Maeder and Shen, 2011). But neuronal subtype identity is revealed as much by distinctions in settling position as surface label (Leone et al., 2008), raising the possibility that neuronal location is a relevant determinant of connectivity.

The connections formed between proprioceptive sensory and motor neurons convey feedback signals that coordinate motor output (Hultborn, 2006). The basic design of this circuit connects the axons of group Ia (muscle spindle) sensory neurons to the cell bodies and dendrites of spinal motor neurons, and does so with an intricate specificity that is evident in the circuits that control hindlimb movement. The fifty or so muscle groups that

© 2011 Elsevier Inc. All rights reserved.

correspondence: tmj1@columbia.edu.

Publisher's Disclaimer: This is a PDF file of an unedited manuscript that has been accepted for publication. As a service to our customers we are providing this early version of the manuscript. The manuscript will undergo copyediting, typesetting, and review of the resulting proof before it is published in its final citable form. Please note that during the production process errors may be discovered which could affect the content, and all legal disclaimers that apply to the journal pertain.

NIH-PA Author Manuscript
NIH-PA Author Manuscript
NIH-PA Author Manuscript

NIH-PA Author Manuscript

NIH-PA Author Manuscript

NIH-PA Author Manuscript

endow the mammalian limb with its modular mechanics are each innervated by a dedicated set of motor neurons, a feature that demands high precision in neuromuscular connectivity (Landmesser, 1978). An even more challenging task faces the sensory neurons that convey feedback from individual muscles: the necessity of forming strong connections with 'self' motor neurons that innervate the same muscle, weaker connections with motor neurons that innervate muscles with synergistic functions, and the avoidance of 'non-self' motor neurons that innervate muscles with irrelevant or opponent functions (Baldissera et al., 1981; Nichols, 1994). The wiring of this connectivity matrix is conserved in limbed vertebrates (Hongo et al., 1984; Mendelson and Frank, 1991), and presumably reflects the critical contribution of sensory feedback pathways to the coordination of movement (Hasan and Stuart, 1988).

The axons of proprioceptive sensory neurons connect with motor neurons late in embryogenesis, days after their peripheral processes have reached limb muscles (Kudo and Yamada 1987; Mears and Frank, 1997). Yet the initial pattern of sensory-motor connectivity generally prefigures the wiring plan evident in the adult (Mears and Frank, 1997; Seebach and Ziskind-Conhaim, 1994). Moreover, the basic pattern of sensory-motor connections is preserved when sensory feedback is silenced through muscle paralysis (Mendelson and Frank, 1991). These observations have led to a view that the specificity of sensory-motor connectivity is hardwired, and that recognition of motor neuron subtype character is a crucial element in the wiring of sensory connections (Ladle et al., 2007). Neurons in different motor pools can be distinguished molecularly, by profiles of transcription factor and surface protein expression (Lin et al., 1998; Price et al., 2002; De Marco Garcia and Jessell, 2008; Livet et al., 2002). But with the notable exception of the involvement of sema3e-plexinD1 signaling in the exclusion of sensory input to a single forelimb motor pool (Pecho-Vrieseling et al., 2009), there has been scant progress in defining the origins of selective sensory-motor connectivity.

The positioning of motor neuron cell bodies in the spinal cord has long been known to exhibit a spatial register with their limb muscle targets. Motor neurons that innervate an individual limb muscle are clustered into spatially coherent 'pools' which occupy stereotypic locations within the spinal cord (Romanes, 1964; Vanderhorst and Holstege, 1997; McHanwell and Biscoe, 1981). There is also a higher-order spatial plan in which motor pools that innervate limb muscles with related functions are themselves grouped together in mini-columns, here termed columels (Figures 1, S1; Romanes 1941, 1951). Intriguingly, the three-dimensional organization of motor columels reflects the position of muscle targets along the three main axes of limb organization (Figure 1). Most strikingly, the dorsoventral position of a motor columel and its resident pools displays a linear correlation with the distal-to-proximal position of its synergistic target muscles (Figures 1B-D, S1; Vanderhorst and Holstege, 1997; Burkholder and Nichols, 2004). The axial registration of motor neuron and muscle position has implications for sensory topography. The peripheral and central endings of proprioceptive sensory neurons connect with muscle and motor neuron respectively, and thus the position of sensory endings along the proximodistal axis of the limb predicts the dorsoventral location and identity of their target motor neurons.

This triangulation of motor, muscle, and sensory coordinates raises the question of whether motor neuron position has any part in the developmental logic that imposes the pattern of sensory-motor connectivity. The specification of motor neuron subtype identity and settling position is directed by a network of Hox transcription factors which assigns profiles of cadherin expression that regulate motor pool clustering (Price et al., 2002; Dasen and Jessell, 2009; Demireva et al., 2011). Thus, inactivation of a motor neuron transcriptional co-factor for Hox proteins, FoxP1, blocks Hox output and strips embryonic motor neurons

NIH-PA Author Manuscript

NIH-PA Author Manuscript

NIH-PA Author Manuscript

of their distinctive pool identities and cadherin profiles (Dasen et al., 2008; Rousso et al., 2008). Although the cell bodies of these 'identity-stripped' motor neurons are dispersed within the ventral spinal cord their axons still project into the limb. But constitutive *FoxP1* mutants die during embryonic development (Wang et al., 2004), too early to assess the impact of motor neuron positional displacement on patterns of sensory-motor connectivity.

We have now generated mice in which *FoxP1* is eliminated selectively from spinal motor neurons, and the viability of this conditional strain has permitted us to examine the contribution of motor neuron position to patterns of sensory-motor connectivity. Despite a profound scrambling of motor neuron position in these mutants, the emergent pattern of monosynaptic sensory-motor connectivity retains a clear dorsoventral positional order. These findings imply that the specificity of sensory-motor connections is achieved, in part, through the ability of sensory axons to project to discrete dorsoventral tiers within the spinal cord in a manner that is independent of motor neuron targets. Thus the settling pattern of motor pools and columels exerts a critical constraint on the final pattern of sensory input specificity.

Results

Motor behavioral defects in *FoxP1$^{MN\Delta}$* Mice

To assess the contribution of motor neuron position to the assembly of sensory-motor connections we set out to eliminate FoxP1 protein expression from motor neurons without affecting other sites of expression. To achieve this, we crossed an *Olig2::Cre* line that targets recombinase expression to motor neuron progenitors (Dessaud et al., 2007) with mice carrying a floxed *FoxP1* allele (Feng et al., 2010; Figure S2A). Analysis of *Olig2::Cre ; FoxP1$^{fl/fl}$* (termed *FoxP1$^{MN\Delta}$*) mutant embryos revealed the absence of FoxP1 protein from spinal motor neurons (Figure S2B), whereas protein expression was preserved in interneurons and non-neural tissues (Figure S2B; data not shown). *FoxP1$^{MN\Delta}$* mice typically survived until at least p60.

The molecular phenotype of motor neurons in e13.5 *FoxP1$^{MN\Delta}$* embryos mimicked that seen in constitutive *FoxP1* mutants. Lumbar level motor neurons retained general transcriptional character, assessed by expression of Isl1/2 (Figure S2B). Expression of the LMC columnar marker retinaldehyde dehydrogenase-2 (RALDH2) was drastically reduced (Figure S2B), together with a loss of motor neurons with a medial (Isl1^{+}, Hb9^{off}) LMC divisional character and the acquisition of an HMC-like (Isl1^{+}, Hb9^{+}) identity (data not shown; Dasen et al., 2008). Nevetheless, as with constitutive *FoxP1* mutants, ~20% of embryonic motor neurons retained lateral (Isl1^{off}, Hb9^{+}, Lhx1^{+}) LMC divisional character (Rousso et al., 2008; data not shown). Despite this, lumbar motor neurons in *FoxP1$^{MN\Delta}$* embryos lacked expression of the definitive motor pool markers Nkx6.1, Nkx6.2, Pea3 and Sema3e (Figure S2B, data not shown; Dasen et al., 2008). Thus, inactivation of motor neuron FoxP1 eradicates molecular features of motor pool differentiation.

We observed a profound impairment in limb coordination during motor behaviors in adult *FoxP1$^{MN\Delta}$* mice (Suppl. Video). On a solid substrate, the fore- and hind-limbs of *FoxP1$^{MN\Delta}$* mice remained extended and were used as paddle-like appendages to propel animals in an undulatory manner (Suppl. Video). These motor behavioral defects did not resolve over time, indicating that *FoxP1$^{MN\Delta}$* mutants are unable to correct their maladaptive behavior through experience (Sperry, 1940).

To resolve whether the behavioral impairment seen in *FoxP1$^{MN\Delta}$* mutants reflects a perturbation in peripheral connectivity we examined the pattern of neuromuscular innervation, focusing on gluteus (GL), tibialis anterior (TA), gastrocnemius (GS) and

NIH-PA Author Manuscript

NIH-PA Author Manuscript

NIH-PA Author Manuscript

intrinsic foot (IF) muscles, which occupy different proximo-distal positions within the hindlimb and serve different biomechanical functions. Analysis of p2 to p21 *FoxP1*$^{MN\Delta}$ mice revealed that limb muscles retained motor innervation, and that the density, size and pattern of acetylcholine receptor plaques at motor end-plates was similar to that observed in wild type mice (Figures 2A; S2C). Thus, the erosion of motor pool identity does not perturb the pattern or stability of neuromuscular connections.

We next performed an electromyographic (EMG) analysis of hindlimb muscle activity patterns in wild type and *FoxP1*$^{MN\Delta}$ mice during a swimming task (Zagoraiou et al., 2009). Recordings from muscles controlling hip [iliopsoas (IP) and GL], knee [vastus lateralis (VL)], and ankle [TA and GS] joints in *FoxP1*$^{MN\Delta}$ mice revealed neurally-evoked bursts of muscle activity (Figure 2B; data not shown). In wild type mice, swimming episodes elicited ipsilateral limb TA and GS bursting in alternating phase, with ipsi- and contralateral limb TA muscles also exhibiting a clear alternation in burst activity (Figure 2B). In *FoxP1*$^{MN\Delta}$ mice, ipsilateral limb TA and GS muscles exhibited short-duration burst activity, but the phase of muscle bursts was synchronous (Figure 2B). In contrast, burst activity in ipsi- and contralateral TA muscles remained in alternating phase (Figure 2B), an indication of the preservation of commissural interneuronal connections that underlie left-right phasing (Kiehn, 2006). The perturbation of EMG activation pattern in FoxP1 mutants implies a change in the intraspinal organization of motor neurons and/or their neural inputs.

Loss of topographic motor mapping in *FoxP1*$^{MN\Delta}$ mice

We examined whether the loss of FoxP1 perturbs the clustering of motor neurons into pools. Our analysis focused on the IF, TA, and GL motor pools, which innervate dorsal muscles at different proximodistal positions, and the GS pool, which innervates a ventral muscle and serves as a cross LMC-divisional counterpart to antagonist TA motor neurons (Figure 1D).

In p21 wild type mice, injection of cholera toxin B (CTB) tracer into the IF, TA, GL or GS muscles labeled clusters of ChAT^{+} motor neurons at stereotypic dorsoventral and rostrocaudal positions (Figure 2C). The IF motor pool was located in an extreme dorsal (tier 1) position at L4-L6, the TA pool was located in a dorsal (tier 2) position at L3-L4, and the GL pool was located in an extreme ventral (tier 4) position at L3-L5 (Figure 2C). The GS pool was detected at the same dorsoventral position as the TA pool, but was situated more medially and extended more caudally, to L5 (Figure 2C). CTB injections targeted to the GS muscle spread to the adjacent biceps femoris (BF) and semitendinosus (ST) hamstring muscles, resulting in a ~30% labeling incidence of BF and ST motor neurons (Figures 2C; S3). Thus in young mice, as in adult cat, the more proximally placed a hindlimb muscle, the more ventrally positioned its cognate LMC motor pool.

In *FoxP1*$^{MN\Delta}$ mice the normal spatial pattern of motor pool and columelar groupings was no longer evident (Figure 2D). In addition there was a systematic ventral shift in the settling position of ChAT^{+} motor neurons, such that at caudal levels the dorsal-most tier 1 domain was devoid of motor neurons (Figure 2D). The only exception to the ventral coherence of limb-innervating motor neurons in *FoxP1*$^{MN\Delta}$ mutants was evident at L3 and rostral L4, where ~25% of motor neurons settled in a more dorsal cluster (termed zone 1), segregated from their ventral (zone 2) neighbors (Figure 2D).

In *FoxP1*$^{MN\Delta}$ mutants we found that the rostro-caudal distribution of CTB-labeled ChAT^{+} motor neurons supplying individual muscles was similar to that in wild type mice (Figure 2D). In contrast the dorsoventral and mediolateral positioning of motor neurons was markedly disrupted. CTB-labeled ‘GL’ and ‘TA’ motor neurons were scattered within zones 1 and 2 (in *FoxP1*$^{MN\Delta}$ mice the designation ‘MN’ indicates that motor pool identity is assigned solely on the basis of muscle target) (Figure 2D; data not shown). Quantitative

NIH-PA Author Manuscript

NIH-PA Author Manuscript

NIH-PA Author Manuscript

analysis of the scattering of 'TA' and 'GL' neurons revealed a distribution close to random (Figure S4; data not shown). The absence of zone 1 from caudal segmental levels meant that virtually all 'IF' motor neurons were detected within zone 2, where they were scattered in random fashion (Figure 2D). More rostrally, CTB-labeled 'GS' (and contaminating 'BF' and 'ST') motor neurons were excluded from zone 1, and scattered within zone 2 (Figures 2D, S4). Thus, zone 1 contains motor neurons that innervate dorsal muscle targets, whereas zone 2 contains a mix of motor neurons innervating dorsal or ventral muscles. The different zonal assignment of motor neurons in *FoxP1*$^{MN\Delta}$ mice likely reflects the population of zone 1 by motor neurons that transiently express lateral LMC divisional character and population of zone 2 by HMC-like motor neurons. This nuance aside, these anatomical studies show that the loss of motor neuron FoxP1 expression degrades the topographic link between motor pool and muscle target.

We next asked whether the density of sensory inputs onto motor neurons is altered in FoxP1 mutants. Sensory boutons were marked by vGluT1 expression and assigned synaptic status on the basis of pre-synaptic expression of bassoon and post-synaptic alignment of shank1a plaques (Figure 3A; Betley et al., 2009). The number of vGluT1^{+} sensory synaptic contacts on the cell body and proximal ~75μm of dendritic arbor of 'TA' and 'GS' motor neurons was similar in p18 wild type and *FoxP1*$^{MN\Delta}$ mice (Figure 3B). Moreover, the growth and patterning of motor neuron dendrites was similar in wild type and *FoxP1*$^{MN\Delta}$, assessed at p0 (Figure S5A,B). Thus, the erosion of subtype identity and mis-positioning of motor neurons does not change the density of sensory inputs or early dendritic pattern.

An anatomical assay of monosynaptic sensory-motor specificity

We next explored the specificity of monosynaptic sensory inputs onto motor neurons supplying different limb muscles. To assess this we devised an anatomical assay that exploits a distinction in sensory transganglionic transport of rhodamine dextran (Rh-Dex) and CTB (Figures 3C; S6). Rh-Dex injected into individual hindlimb muscles is taken up by proprioceptive sensory axons but is not transported transganglionically, whereas CTB is transported into the central branch of the sensory axon, and accumulates in vGluT1^{+} sensory bouton contacts with CTB-labeled motor neurons (Figure S6). So after Rh-Dex and CTB injection into different muscles in wild type mice, comparison of the density of CTB-labeled vGluT1^{+} sensory bouton contacts with CTB or Rh-Dex labeled motor neurons at p21 provides an indication of the incidence of on-target 'self' and off-target 'non-self' sensory-motor connections. We excluded γ-motor neurons from our analysis since this set of motor neurons lacks sensory input. γ-motor neurons, identified by their small size, bipolar morphology and expression of the transcription factor Err3 (Friese et al., 2009), were detected at similar incidence in wild type and *FoxP1*$^{MN\Delta}$ mice (Figure S5, C-F).

We used this connectivity assay to monitor the specificity of 'self' sensory-motor connections within the GL, TA, IF and GS reflex arcs in wild type mice. After CTB injection into individual muscles we found that 85-100% of the motor neurons within an individual pool received synaptic inputs from sensory afferents supplying the same muscle (Figures 3D,F,H; S7). Typically, ~30-50% of the total population of vGluT1^{+} bouton contacts derived from 'self' sensory afferents (Figure 3H). Incomplete CTB labeling of sensory boutons stems, in part, from the fact that ~30% of all monosynaptic inputs to motor neurons derive from sensory afferents supplying synergistic muscles (Brown, 1981). Thus transganglionic transport of CTB efficiently labels sensory boutons on 'self' motor neurons.

We used dual CTB/Rh-Dex labeling to examine the specificity of group Ia sensory connections with 'non-self' motor neurons that occupy different dorsoventral tiers. After pairing GL CTB with TA or IF Rh-Dex injections in wild type mice, we found that GL sensory boutons never contacted TA or IF motor neurons (Figure 3E,I). Conversely, pairing

NIH-PA Author Manuscript

NIH-PA Author Manuscript

NIH-PA Author Manuscript

TA CTB and GL Rh-Dex muscle injections revealed that none of the GL motor neurons were contacted by TA sensory boutons (Figure 3G,I; data not shown). These findings provide evidence that sensory afferents fail to form monosynaptic connections with motor pools that occupy different dorsoventral tiers. We also analyzed the selectivity with which sensory afferents supplying an individual muscle form connections with antagonist motor neurons that occupy the same dorsoventral tier position. After TA muscle CTB and GS muscle Rh-Dex injection, GS motor neurons were never contacted by TA sensory boutons (Figure 3I). Conversely, pairing GS muscle CTB and TA muscle Rh-Dex injection revealed that none of the TA motor neurons were contacted by GS (or BF and ST) sensory boutons (Figure 3I). Thus, sensory afferents fail to form connections with antagonist motor neurons within the same dorsoventral tier. The selectivity of connections revealed anatomically in mouse is in close agreement with physiological studies of patterns of monosynaptic connectivity.

Degraded specificity of sensory-motor connections in *FoxP1$^{MN\Delta}$* mice

The fidelity of this connectivity assay permitted us to examine how the pattern of sensory-motor connections changes under conditions in which motor neuron position is disrupted.

We focused first on the specificity of connections in the TA and GL reflex arcs, given the distinction in dorsoventral position of these two motor pools in wild type mice. We first analyzed the impact of FoxP1 inactivation on the incidence of 'self' sensory-motor connections. After TA muscle CTB injection, 56% of 'TA' motor neurons received TA sensory input, a one third reduction compared to wild type values (Figures 4A; S7). Of the total population of sensory boutons on homonymous 'TA' motor neurons, 33% derived from TA afferents, again a one third reduction compared to values in wild type mice (Figure 4A; S7). Conversely, after GL muscle CTB injection we found that 45% of all 'GL' motor neurons received GL sensory input, a ~2-fold reduction compared to wild type values (Figures 4B; S7). Of the total population of sensory bouton contacts on 'GL' motor neurons, 16% derived from GL afferents, again a ~2-fold reduction compared to wild type values (Figure 4B; S7). Thus the incidence of 'self' sensory-motor connections in the TA and GL reflex arcs is reduced in *FoxP1$^{MN\Delta}$* mice. A reduction in sensory innervation of 'self' motor neurons was observed for other reflex arcs examined (Figure S7).

We also examined the incidence of ectopic sensory-motor connections in the TA and GL reflex arcs in FoxP1 mutants. We found that 50% of 'GL' motor neurons now received TA sensory input, and that 30% of all sensory bouton contacts with 'GL' motor neurons derived from TA afferents -- an illicit 'non-self' input pattern (Figure 4A, C). Conversely, we found that 56% of 'TA' motor neurons received GL sensory input, and that 19% of all sensory bouton contacts with 'TA' motor neurons derived from GL afferents -- again an ectopic 'non-self'connectivity pattern (Figure 4B,D). Thus the exclusivity of sensory-motor connections normally observed in the TA and GL reflex arcs is eroded in *FoxP1$^{MN\Delta}$* mice, such that sensory afferents innervate 'self' and 'non-self' motor neurons at similar incidence.

A dorsoventral constraint on sensory-motor connectivity in *FoxP1$^{MN\Delta}$* mice

The marked reduction in the number of motor neurons in receipt of 'self' sensory inputs in FoxP1 mutants led us to consider whether the dorsoventral position of a motor neuron might be a factor in determining its sensory innervation status. To assess this, we analyzed the position of innervated and uninnervated 'TA' and 'GL' motor neurons in *FoxP1$^{MN\Delta}$* mice (Figure 4E). We found that 96% of all 'TA' motor neurons in receipt of TA sensory bouton contacts occupied a dorsal (zone 1) position that coincided with the normal settling domain of wild type TA motor neurons (Figure 4F,G). Similarly, 100% of 'GL' motor neurons in

NIH-PA Author Manuscript

NIH-PA Author Manuscript

NIH-PA Author Manuscript

receipt of TA sensory bouton contacts were confined to this same zone 1 domain (Figure 4F,G). For these dorsal 'TA' and 'GL' neurons, 54% and 56% respectively, of all sensory bouton contacts derived from TA afferents (Figure S7). Thus in FoxP1 mutants, TA sensory afferents form preferential synaptic contacts with motor neurons located at a dorsoventral position that coincides with the location of wild type TA motor neurons, regardless muscle target.

Analysis of the impact of position on motor neuron innervation status by GL sensory afferents revealed that 96% of all 'GL' motor neurons contacted by GL sensory boutons were confined to a ventral zone 2 domain that coincided with the position of wild type GL motor neurons (Figure 4G). Similarly, 100% of 'TA' motor neurons that received GL sensory contacts were confined to this same ventral domain (Figure 4G). For this set of ventrally located 'GL' and 'TA' motor neurons, 30% and 28% of all bouton contacts derived from GL afferents (Figure 4G; S7). Thus in FoxP1 mutants, sensory afferents supplying an individual muscle exhibit a striking preference for motor neurons occupying a dorsoventral position that coincides with the normal tier location of their 'self' motor pool.

Sensory targeting in the absence of motor neurons

The ability of sensory afferents to target specific dorsoventral domains without regard for motor neuron subtype character raised the issue of whether sensory tier targeting also occurs in the absence of motor neurons. For this analysis we focused on the trajectory of IF sensory afferents that normally project to a dorsal tier 1 domain that now lacks motor neurons (Figure 5A, C). In *FoxP1*$^{MN\Delta}$ mice, none of the ventrally-displaced' IF' motor neurons received input from IF sensory afferents, although they were contacted by GL sensory afferents, consistent with the preservation of their ventral projection domain (Figure 5D-G). These observations led us to define in more detail, the termination pattern of IF sensory afferents in FoxP1 mutants. In contrast to p21 wild type mice, where sensory boutons were detected on the cell bodies and dendrites of IF motor neurons within and dorsomedial to the tier 1 domain (Figure 5B,H), labeled IF boutons in FoxP1 mutants were virtually absent from tier 1, and instead were concentrated in a more dorsomedial position, where they contacted interneurons (Figure 5I,J).

Do IF sensory afferents initially project to tier 1 in FoxP1 mutants, and only later retract from this motor neuron-free domain? Rh-Dex labeling of L5 dorsal roots was used to monitor the intraspinal trajectory of embryonic (e18) sensory afferents. Analysis of wild type embryos revealed a prominent sensory afferent fascicle that projected laterally towards the cell bodies and dendrites of IF motor neurons within tier 1 (Figure 5K). Even at this early stage very few labeled sensory axons were detected more ventrally (Figure 5K). In *FoxP1*$^{MN\Delta}$ embryos, a similarly oriented sensory afferent fascicle reached tier 1, even though this dorsal domain was devoid of motor neurons (Figure 5L). These data provide evidence that sensory afferents project to their tier domain in the absence of target motor neurons, although the maintenance of sensory axon termination fields appears dependent on the presence of motor neurons.

Erosion of antagonist specificity in *FoxP1*$^{MN\Delta}$ mice

Finally, we examined whether the stringent exclusion of sensory connections with 'non-self' antagonist motor neurons evident in wild type mice is also eroded by the loss of FoxP1. After GS muscle CTB and TA muscle Rh-Dex injections in *FoxP1*$^{MN\Delta}$ mice and analysis at p21, 54% of 'TA' motor neurons received GS [and presumably BF and ST] sensory input (Figure 6A; S7), a novel connectivity pattern that reflects a breakdown in the avoidance of sensory connections with antagonist motor neurons.

NIH-PA Author Manuscript

NIH-PA Author Manuscript

NIH-PA Author Manuscript

In contrast, after TA muscle CTB and GS muscle Rh-Dex injections in *FoxP1*$^{MN\Delta}$ mice, 'GS' (and 'BF' and 'ST') motor neurons still failed to receive TA sensory input (Figure 6B). This finding reflects the fact that TA sensory afferents are restricted to a dorsal domain in *FoxP1*$^{MN\Delta}$ mice, and thus never invade the ventral domain that contains 'GS' motor neurons. Thus, the erosion of antagonist exclusion in FoxP1 mutants is constrained by the dorsoventral restriction in sensory projection pattern. Together, these findings indicate that motor neuron position is a key arbiter of the profiles of 'self'and 'non-self' sensory connectivity.

Discussion

Sensory-motor reflex circuits are constructed with high specificity, but just how sensory axons sift through a diverse array of potential motor neuron targets to select their synaptic partners remains unclear. Our findings indicate that the numerical challenge posed by the matrix of sensory-motor connectivity is met by deconstructing the specificity problem into a series of modular programs. In the first of these, sensory afferents supplying individual limb muscles target discrete dorsoventral tiers without reliance on recognition of motor neuron subtype. By implication, the dorsoventral settling position of motor neurons is a significant determinant of sensory input specificity. In many brain regions, neurons are clustered into stereotypic nuclear groups, raising the possibility that neuronal position contributes to circuit assembly in other regions of the mammalian CNS.

Sensory tier targeting provides a purpose for motor neuron columelar organization

The columelar organization of spinal motor neurons mirrors, with remarkable fidelity, the primary axes of limb construction (Romanes, 1951). This topographic arrangement presumably reflects the demand that the spinal motor system tailor itself to fit an independently-assigned and non-negotiable set of mechanical constraints on limb movement (Nichols, 1994). But the merits of organizing motor neurons with this high degree of spatial order have remained obscure. Our findings on sensory tier targeting provide a partial explanation for the puzzle of motor neuron position – they argue that the precise positioning of motor columels ensures that functionally-related motor neurons are strategically placed to receive the coordinating influence of proprioceptive sensory feedback.

The existence of a target-independent step in the wiring of sensory-motor connections has precedent. In limbs deprived of muscle, motor nerve branching patterns are largely preserved, implying that target muscle itself contributes little to the selectivity of motor innervation (Lewis et al., 1981; Phelan and Hollyday, 1990). Instead, neuromuscular connectivity patterns are imposed by limb mesenchymal signals that coordinate the pattern of muscle cleavage and the trajectory of motor axons (Landmesser, 1978; Kardon et al., 2003), such that motor axons have little choice but to connect with the nascent muscle that awaits their arrival. In addition, analysis of primary sensory projection patterns in the ventral nerve cord of *Drosophila* have shown that dorsoventral and mediolateral sensory termination domains are set by target-independent signaling gradients – mediated by slits and semaphorins, respectively (Zlatic et al., 2009). Thus, key steps in sensory-motor circuit assembly are accomplished without recognition of target cell subtype in vertebrates and invertebrates. The source and identity of motor neuron-independent cues that guide sensory axons to specific dorsoventral tiers in the spinal cord remain unclear. A ventral source of signals, perhaps semaphorins (Messersmith et al., 1995), could repel or attract group Ia sensory afferents, with differential axonal responses underlying sensory targeting to different tiers. Alternatively, tier-specific radial glial signaling (Hochstim et al., 2008) could restrict sensory afferents to discrete dorsoventral domains.

NIH-PA Author Manuscript

NIH-PA Author Manuscript

NIH-PA Author Manuscript

More generally, our findings pose the question of the benefit of constructing spinal motor circuits through a mechanism that couples the precise positioning of neuronal cell bodies to the target-independence of input projections. Spinal interneuron subtypes involved in patterning motor output also settle at distinct dorsoventral positions (Goulding, 2009), and the differing tier projection domains of sensory afferent supplying limb muscles will likely constrain connectivity with interneurons as well as motor neurons. One virtue of relying on a connectivity logic based on position is that it permits sensory afferents to engage, coordinately, the many interneuron subtypes allocated to the firing of a single motor pool, without the molecular burden of allocating matching surface labels to each contributing neuronal type.

Columelar coordinates for connectivity: caveats and concerns

Tier targeting emphasizes the idea that motor neuron cell body position is a determinant of sensory connectivity patterns. Yet the majority of sensory inputs are located on the dendrites of mature motor neurons (Brown, 1981), a finding seemingly at odds with the implied significance of somatic coordinates. Initially, however, sensory synapses are concentrated on perisomatic regions of mammalian motor neurons, and only later are redistributed to dendritic locations (Gibson and Clowry, 1999; Ronnevi and Conradi, 1974). Moreover in rodents, embryonic sensory axons appear to ignore motor neuron dendrites that intersect their ventrally-oriented path, elaborating terminal varicosities only in the vicinity of cell bodies, (Snider et al., 1992). Parallel physiological studies have detected monosynaptic sensory-motor connections only when proprioceptive axons reach motor neuron cell bodies (Kudo and Yamada, 1987), supporting the idea that columelar coordinates constrain the pattern of sensory-motor connections.

Although most sensory afferents form synapses exclusively with motor pools that occupy a single dorsoventral tier, there are exceptions to this general rule – sensory afferents conveying information from hip and ankle muscles innervate motor neurons controlling knee muscles (Eccles et al., 1957; Hongo et al., 1984; Nichols et al., 2002). Such instances of trans-tier connectivity could originate with differences in developmental timing - the dendrites of neurons in certain motor pools may have extended into adjacent tier territories prior to sensory axonal invasion, permitting input from afferents programmed to target these adjacent tiers.

Sensory tier targeting and limb positional coordinates

Sensory tier targeting provides a rationale for arranging motor neurons into columelar groups, but does not explain the higher order register between relative columelar position and limb axial coordinates. This spatial link could have its basis in the developmental programming of proprioceptive sensory subtype character. In this view, the proximodistal position occupied by proprioceptive sensory endings would expose them to mesenchymal signals that confer the subtype identities needed to direct their intraspinal trajectory and dorsoventral termination domain. The peripheral endings of group Ia sensory axons are in place well before their central axons enter the ventral spinal cord, and thus limb-derived positional signals have ample time to impose subtype character on sensory neurons. Indeed, embryological studies in chick have provided some evidence that limb signals can direct selective sensory-motor connectivity (Wenner and Frank, 1995).

Intriguingly, the topographic matching of motor neuron columelar groups and limb muscles may have a common molecular foundation. Motor neuron subtype identities that direct dorsoventral and mediolateral settling position are initiated by the early opponent actions of retinoid and FGF signaling systems and interpreted by a combinatorial network of Hox genes and FoxP co-factors (Dasen and Jessell, 2009). In parallel, the early proximodistal

NIH-PA Author Manuscript

NIH-PA Author Manuscript

NIH-PA Author Manuscript

pattern of the limb mesenchyme is established by opponent retinoid and FGF signaling, and mediated by the localized expression of Hox genes and their cofactors (Cooper et al., 2011; Rosello-Diez et al., 2011). The coordinated activities of Hox cluster genes may therefore assign matching spinal and limb positional values that later direct the pattern of sensory-motor connections.

Beyond tier targeting: unresolved programs of sensory-motor connectivity

We emphasize that the tier targeting strategy uncovered through analysis of FoxP1 mutants provides only a partial solution to the sensory-motor connectivity problem. On arrival at a designated tier destination, group Ia sensory afferents avoid motor neurons that innervate antagonist muscles at the same joint and, in addition, establish weighted inputs to motor pools within a columel.

The avoidance of antagonist motor neurons could involve recognition of a binary motor neuron divisional character, given that pools that control muscles with antagonist functions are typically segregated into columels occupying opponent medial and lateral divisions of the LMC. Alternatively, and akin to the situation in *Drosophila* (Zlatic et al., 2009), a motor neuron-independent program of mediolateral sensory targeting could underlie the avoidance of neurons in antagonist columels. Scrambling motor neuron position while maintaining transcriptional distinctions in divisional identity (see Demireva et al., 2011) could help to resolve these possibilities. It is also unclear how the variably weighted sensory connections with motor pools within a columel are established. Patterns of sensory-motor connectivity across the pools of an individual columelar group are altered after silencing sensory feedback (Mendelson and Frank, 1991), raising the possibility that sensory weighting is achieved through activity-mediated refinement of connections.

Regardless of precise mechanism, our findings suggest that the complex sensory challenge of selecting the right motor pools as synaptic partners has been met by deconstructing this larger problem into a series of simpler cellular interactions, each of which presents sensory axons with a more limited set of choices. Dorsoventral sensory tier targeting arguably simplifies connection complexity by a factor of four, and the settling of motor neurons at different mediolateral and rostrocaudal positions may similarly reduce the complexity of sensory connectivity. Which of these modular steps actually involves recognition of motor neuron subtype label is an intriguing question.

Experimental Procedures

Mouse Strains

Olig2::Cre (Dessaud et al., 2008) and conditional *FoxP1* (Feng et al., 2010) strains have been described. > 60 conditional mutant mice were analyzed in this study.

Immunohistochemistry

Immunohistochemical labeling was performed as described (Betley et al., 2009), using FITC-, Cy3-, Cy5-, or Alexa 488- reagents. Images were acquired on a Zeiss LSM-510 Meta confocal microscope. Primary antibodies and reagents included in supplementary text.

Plotting Holstege-Nichols linearity

The dorsoventral position of motor pools and columels was plotted as a function of the proximodistal position of hindlimb muscles. The epicenter of individual lumbar motor pools was determined from data in Vanderhorst and Holstege (1997), and expressed as distance from ventral limit of spinal gray matter. The proximodistal position of cat hindlimb muscles

NIH-PA Author Manuscript

NIH-PA Author Manuscript

NIH-PA Author Manuscript

was calculated from muscle origin and insertion point data in Burkholder and Nichols (2004), assigning pelvis position as the origin.

Motor and sensory neuron labeling

Ventral root fills were performed on p0-7 mice. For retrograde tracing motor neurons, TMR-Dextran (Rh-Dex) was applied to ventral roots with overnight incubation in oxygenated ACSF before fixation. Motor neurons were retrogradely labeled *in vivo* by intramuscular injection of cholera toxin B subunit (CTB), CTB-Alexa^{488} or CTB-Alexa^{555} or Rh-Dextran (Shneider et al., 2009). Dorsal root fills were performed as described (Pecho-Vrieseling et al., 2009).

Quantification of sensory synaptic contacts with motor neurons

Quantification of vGluT1^{+} sensory bouton contacts with p18-21 motor neuron somata and ~75μm proximal dendritic arbor was performed using 0.5μm confocal z-scans of 30 to 60μm thick sections. γ-motor neurons were excluded from analysis. Motor neuron surface area was determined using Neurolucida. Synaptic bouton density was determined from 0.7μm confocal images using a Zen tiling function (Zeiss). Images were analyzed with IMARIS software (Bitplane) and synapses marked using IMARIS Coloc, filtered for size using a SPOTS function. Coordinate position and density algorithms of labeled synapses were calculated in MATLAB. Data are representations as mean and +/- standard deviation can be found in supplementary materials.

EMG recordings

We performed EMG recordings during a swimming task that provides enhanced buoyancy in *FoxP1^{fl}* and *FoxP1$^{MN\Delta}$* mice (Suppl. Video) (Zagoraiou et al., 2009).

Quantitative analysis of motor neuron positioning

Motor neurons were labeled by muscle CTB injection and their position assessed in 30-40 μm vibratome sections from *FoxP1^{fl}* and *FoxP1$^{MN\Delta}$* mice. The summed pair-wise Euclidean distance between CTB-labeled motor neurons was compared with a random distribution generated by 200 shuffled permutations of the location of the CTB-labeled neurons. Z scores indicate the number of standard deviations from the mean of the random distribution.

Supplementary Material

Refer to Web version on PubMed Central for supplementary material.

Acknowledgments

We thank George Romanes for enlightening discussions on motor neuron groupings, Jeremy Dasen for insight into FoxP function, Joriene De Noiij for help with dorsal root fills, Gert Holstege for motor pool maps, Julia Kaltschmidt for contributions to the design of sensory-motor specificity assays, Tim Machado for statistical analysis of neuronal distributions, Richard Nichols and Trevor Drew for insight into limb biomechanics, John Kelly for detective work, Kendall Doerr for a sense of place, and Ira Schieren for assistance with figures and graphics. Kaity Miao, Monica Mendelsohn, June Harriss and Deborah Surman helped in mouse genotyping and husbandry. Silvia Arber, Richard Axel, Jeremy Dasen, Joriene de Nooij; Chris Henderson, John Kelly, George Mentis, Richard Nichols, Sebastian Poliak and George Romanes provided helpful comments on the manuscript. GS was supported by the Gatsby Charitable Foundation, PWT by NIH grant R01-CA31534 and the Marie Betzer Morrow endowment. TMJ is an Investigator of the Howard Hughes Medical Institute and was supported by NIH grants R01-NS033245 and P01-NS055923, ProjectALS/P^{2}ALS, The Wellcome Trust, NYSTEM and The Harold and Leila Mathers Foundation.

NIH-PA Author Manuscript

NIH-PA Author Manuscript

NIH-PA Author Manuscript

References

Baldissera, F.; Hultborn, H.; Illert, M. Integration in spinal neuronal systems. In: Brooks, VB., editor. Handbook of Physiology, The Nervous System. 1981. p. 509-595.

Betley JN, Wright CV, Kawaguchi Y, Erdélyi F, Szabó G, Jessell TM, Kaltschmidt JA. Stringent specificity in the construction of a GABAergic presynaptic inhibitory circuit. Cell. 2009; 139:161–174. [PubMed: 19804761]

Brown, AG. Organization in the spinal cord. Springer Verlag; 1981. p. 238

Burkholder TJ, Nichols TR. Three-dimensional model of the feline hindlimb. J Morphol. 2004; 261:118–129. [PubMed: 15164372]

Cooper KL, Hu JK, ten Berge D, Fernandez-Teran M, Ros MA, Tabin CJ. Initiation of proximo-distal patterning in the vertebrate limb by signals and growth. Science. 2011; 332:1083–1086. [PubMed: 21617075]

Dasen JS, De Camilli A, Wang B, Tucker PW, Jessell TM. Hox repertoires for motor neuron diversity and connectivity gated by a single accessory factor, FoxP1. Cell. 2008; 134:304–316. [PubMed: 18662545]

Dasen JS, Jessell TM. Hox networks and the origins of motor neuron diversity. Curr Top Dev Biol. 2009; 88:169–200. [PubMed: 19651305]

De, Marco; Garcia, NV.; Jessell, TM. Early motor neuron pool identity and muscle nerve trajectory defined by postmitotic restrictions in Nkx6.1 activity. Neuron. 2008; 57:217–231. [PubMed: 18215620]

Demireva E, Shapiro LS, Jessell TM, Zampieri N. Motor neuron position and topographic order imposed by β- and γ-catenin activities. Cell. 2011 In Press.

Dessaud E, Yang LL, Hill K, Cox B, Ulloa F, Ribeiro A, Mynett A, Novitch BG, Briscoe J. Interpretation of the sonic hedgehog morphogen gradient by a temporal adaptation mechanism. Nature. 2007; 450:717–720. [PubMed: 18046410]

Eccles JC, Eccles RM, Lundberg A. The convergence of monosynaptic excitatory afferents on to many different species of alpha motoneurones. J Physiol. 1957; 137:22–50. [PubMed: 13439582]

Feng X, et al. Foxp1 is an essential transcriptional regulator for the generation of quiescent naive T cells during thymocyte development. Blood. 2010; 115:510–518. [PubMed: 19965654]

Friese A, Kaltschmidt JA, Ladle DR, Sigrist M, Jessell TM, Arber S. Gamma and alpha motor neurons distinguished by expression of transcription factor Err3. Proc Natl Acad Sci U S A. 2009; 106:13588–13593. [PubMed: 19651609]

Gibson CL, Clowry GJ. Retraction of muscle afferents from the rat ventral horn during development. Neuroreport. 1999; 10:231–235. [PubMed: 10203314]

Goulding M. Circuits controlling vertebrate locomotion: moving in a new direction. Nat Rev Neurosci. 2009; 10:507–518. [PubMed: 19543221]

Hasan Z, Stuart DG. Animal solutions to problems of movement control: the role of proprioceptors. Ann Rev Neurosci. 1988; 11:199–223. [PubMed: 3284440]

Hochstim C, Deneen B, Lukaszewicz A, Zhou Q, Anderson DJ. Identification of positionally distinct astrocyte subtypes whose identities are specified by a homeodomain code. Cell. 2008; 133:510–522. [PubMed: 18455991]

Hongo T, Lundberg A, Phillips CG, Thompson RF. The pattern of monosynaptic Ia-connections to hindlimb motor nuclei in the baboon: a comparison with the cat. Proc R Soc Lond B Biol Sci. 1984; 221:261–289. [PubMed: 6146138]

Hultborn H. Spinal reflexes, mechanisms and concepts: from Eccles to Lundberg and beyond. Prog Neurobiol. 2006; 78:215–232. [PubMed: 16716488]

Kardon G, Harfe BD, Tabin CJA. Tcf4-positive mesodermal population provides a prepattern for vertebrate limb muscle patterning. Dev Cell. 2003; 5:937–944. [PubMed: 14667415]

Kiehn O. Locomotor circuits in the mammalian spinal cord. Ann Rev Neurosci. 2006; 29:279–306. [PubMed: 16776587]

Kudo N, Yamada T. Morphological and physiological studies of development of the monosynaptic reflex pathway in the rat lumbar spinal cord. J Physiol. 1987; 389:441–459. [PubMed: 2824763]

NIH-PA Author Manuscript

NIH-PA Author Manuscript

NIH-PA Author Manuscript

Ladle DR, Pecho-Vrieseling E, Arber S. Assembly of motor circuits in the spinal cord: driven to function by genetic and experience-dependent mechanisms. Neuron. 2007; 56:270–283. [PubMed: 17964245]

Landmesser L. The distribution of motoneurones supplying chick hind limb muscles. J Physiol. 1978; 284:371–389. [PubMed: 731549]

Leone DP, Srinivasan K, Chen B, Alcamo E, McConnell SK. The determination of projection neuron identity in the developing cerebral cortex. Curr Opinion Neurobiol. 2008; 18:28–35.

Lewis J, Chevallier A, Kieny M, Wolpert L. Muscle nerve branches do not develop in chick wings devoid of muscle. J Embryol Exp Morphol. 1981; 64:211–232. [PubMed: 7310301]

Lin JH, Saito T, Anderson DJ, Lance-Jones C, Jessell TM, Arber S. Functionally related motor neuron pool and muscle sensory afferent subtypes defined by coordinate ETS gene expression. Cell. 1998; 95:393–407. [PubMed: 9814709]

Livet J, Sigrist M, Stroebel S, De Paola V, Price SR, Henderson CE, Jessell TM, Arber S. ETS gene Pea3 controls the central position and terminal arborization of specific motor neuron pools. Neuron. 2002; 35:877–892. [PubMed: 12372283]

Maeder CI, Shen K. Genetic dissection of synaptic specificity. Curr Opin Neurobiol. 2011; 21:93–99. [PubMed: 21087855]

McHanwell S, Biscoe TJ. The localization of motoneurons supplying the hindlimb muscles of the mouse. Philos Trans R Soc Lond B Biol Sci. 1981; 293:477–508. [PubMed: 6115428]

Mears SC, Frank E. Formation of specific monosynaptic connections between muscle spindle afferents and motoneurons in the mouse. J Neurosci. 1997; 17:3128–3135. [PubMed: 9096147]

Mendelson B, Frank E. Specific monosynaptic sensory-motor connections form in the absence of patterned neural activity and motoneuronal cell death. J Neurosci. 1991; 11:1390–1403. [PubMed: 2027053]

Messersmith EK, Leonardo ED, Shatz CJ, Tessier-Lavigne M, Goodman CS, Kolodkin AL. Semaphorin III can function as a selective chemorepellent to pattern sensory projections in the spinal cord. Neuron. 1995; 14:949–59. [PubMed: 7748562]

Nichols TR. A biomechanical perspective on spinal mechanisms of coordinated muscular action: an architecture principle. Acta Anat (Basel). 1994; 151:1–13. [PubMed: 7879588]

Nichols, TR.; Wilmink, RJH.; Burkholder, TJ. The multidimensional and temporal regulation of limb mechanics by spinal circuits. In: Latash, ML., editor. Progress in Motor Control. 2002. p. 179-193.

Pecho-Vrieseling E, Sigrist M, Yoshida Y, Jessell TM, Arber S. Specificity of sensory-motor connections encoded by Sema3e-Plxnd1 recognition. Nature. 2009; 11:842–846. [PubMed: 19421194]

Phelan KA, Hollyday M. Axon guidance in muscleless chick wings: the role of muscle cells in motoneuronal pathway selection and muscle nerve formation. J Neurosci. 1990; 10:2699–2716. [PubMed: 2167355]

Price SR, De Marco Garcia NV, Ranscht B, Jessell TM. Regulation of motor neuron pool sorting by differential expression of type II cadherins. Cell. 2002; 109:205–216. [PubMed: 12007407]

Romanes GJ. Cell columns in the spinal cord of a human foetus of fourteen weeks. J Anat. 1941; 75:145–152. [PubMed: 17104847]

Romanes GJ. The motor cell columns of the lumbo-sacral spinal cord of the cat. J Comp Neurol. 1951; 94:313–363. [PubMed: 14832391]

Romanes GJ. The motor pools of the spinal cord. Prog Brain Res. 1964; 11:93–119. [PubMed: 14300484]

Ronnevi LO, Conradi S. Ultrastructural evidence for spontaneous elimination of synaptic terminals on spinal motoneurons in the kitten. Brain Res. 1974; 80:335–339. [PubMed: 4417941]

Roselló-Díez A, Ros MA, Torres M. Diffusible signals, not autonomous mechanisms, determine the main proximodistal limb subdivision. Science. 2011; 332:1086–1088. [PubMed: 21617076]

Rousso DL, Gaber ZB, Wellik D, Morrisey EE, Novitch BG. Coordinated actions of the forkhead protein Foxp1 and Hox proteins in the columnar organization of spinal motor neurons. Neuron. 2008; 59:226–240. [PubMed: 18667151]

NIH-PA Author Manuscript

NIH-PA Author Manuscript

NIH-PA Author Manuscript

Seebach BS, Ziskind-Conhaim L. Formation of transient inappropriate sensorimotor synapses in developing rat spinal cords. J Neurosci. 1994; 14:4520–4528. [PubMed: 8027791]

Shneider NA, Mentis GZ, Schustak J, O'Donovan MJ. Functionally reduced sensorimotor connections form with normal specificity despite abnormal muscle spindle development: the role of spindle-derived neurotrophin 3. J Neurosci. 2009; 29:4719–4735. [PubMed: 19369542]

Snider WD, Zhang L, Yusoof S, Gorukanti N, Tsering C. Interactions between dorsal root axons and their target motor neurons in developing mammalian spinal cord. J Neurosci. 1992; 12:3494–3508. [PubMed: 1326607]

Sockanathan S, Jessell TM. Motor neuron-derived retinoid signaling specifies the subtype identity of spinal motor neurons. Cell. 1998; 94:503–514. [PubMed: 9727493]

Sperry RW. The functional results of muscle transposition in the hind limb of the rat. J Comp Neurology. 1940; 73:379–404.

Stevens CF. Neuronal diversity: too many cell types for comfort. Current Biology. 1998; 8:R708–R710. [PubMed: 9778523]

Vanderhorst VG, Holstege G. Organization of lumbosacral motoneuronal cell groups innervating hindlimb, pelvic floor, and axial muscles in the cat. J Comp Neurol. 1997; 382:46–76. [PubMed: 9136811]

Wang B, Weidenfeld J, Lu MM, Maika S, Kuziel WA, Morrisey EE, Tucker PW. Foxp1 regulates cardiac outflow tract, endocardial cushion morphogenesis and myocyte proliferation and maturation. Development. 2004; 131:4477–4487. [PubMed: 15342473]

Wenner P, Frank E. Peripheral target specification of synaptic connectivity of muscle spindle sensory neurons with spinal motoneurons. J Neurosci. 1995; 15:8191–8198. [PubMed: 8613753]

Zagoraiou L, Akay T, Martin JF, Brownstone RM, Jessell TM, Miles GB. A cluster of cholinergic premotor interneurons modulates mouse locomotor activity. Neuron. 2009; 64:645–662. [PubMed: 20005822]

Zlatic M, Li F, Strigini M, Grueber W, Bate M. Positional cues in the Drosophila nerve cord: semaphorins pattern the dorso-ventral axis. PLoS Biol. 2009; 7:e1000135. [PubMed: 19547742]

NIH-PA Author Manuscript

NIH-PA Author Manuscript

NIH-PA Author Manuscript

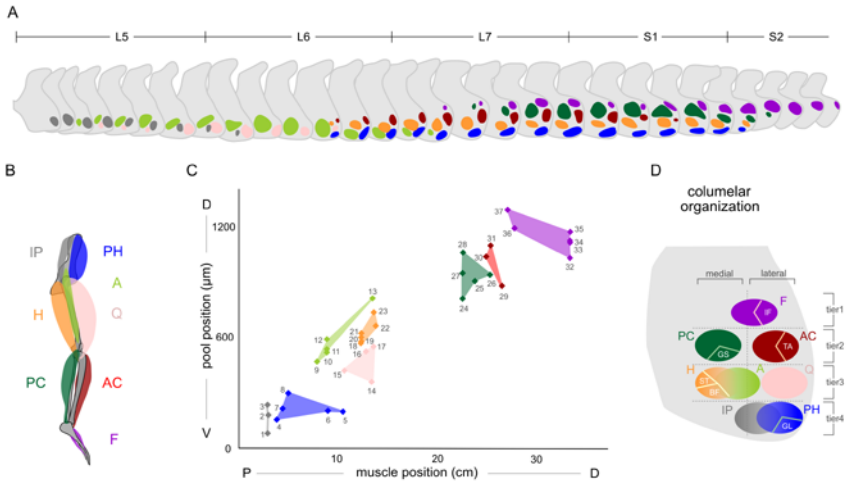

Figure 1. Motor neuron columelar organization

A. Motor columels in cat lumbar spinal cord. Color code: dark blue/ proximal hip (PH), gray/ iliopsoas (IP), light green/adductors (A), pink/quadriceps (Q), orange/ hamstring (H), red/anterior crural (AC), dark green/posterior crural (PC), purple/ foot (F). Lumbar (L) and sacral (S) segmental levels are indicated. Derived from data in Vanderhorst and Holstege (1997).

B. The proximodistal organization of muscles in cat hindlimb.

C. The dorsoventral (DV, µm) position of motor pools in cat lumbar spinal cord and the proximodistal (PD, cm) position of muscles in cat hindlimb. Color code as in A. Colored fields represent columelar/synergy groups, and individual points mark specific motor pools and limb muscles. Muscle and motor neuron key provided in supplementary text. Motor pool position from Vanderhorst and Holstege (1997), muscle position from Burkholder and Nichols (2004).

D. Columelar organization along the dorsoventral axis, after rostrocaudal compression into 2-dimensions. Columels are assigned to dorsoventral tiers that correspond to muscles at individual joints. The approximate position of relevant motor pools within columelar groups is marked.

NIH-PA Author Manuscript
NIH-PA Author Manuscript
NIH-PA Author Manuscript

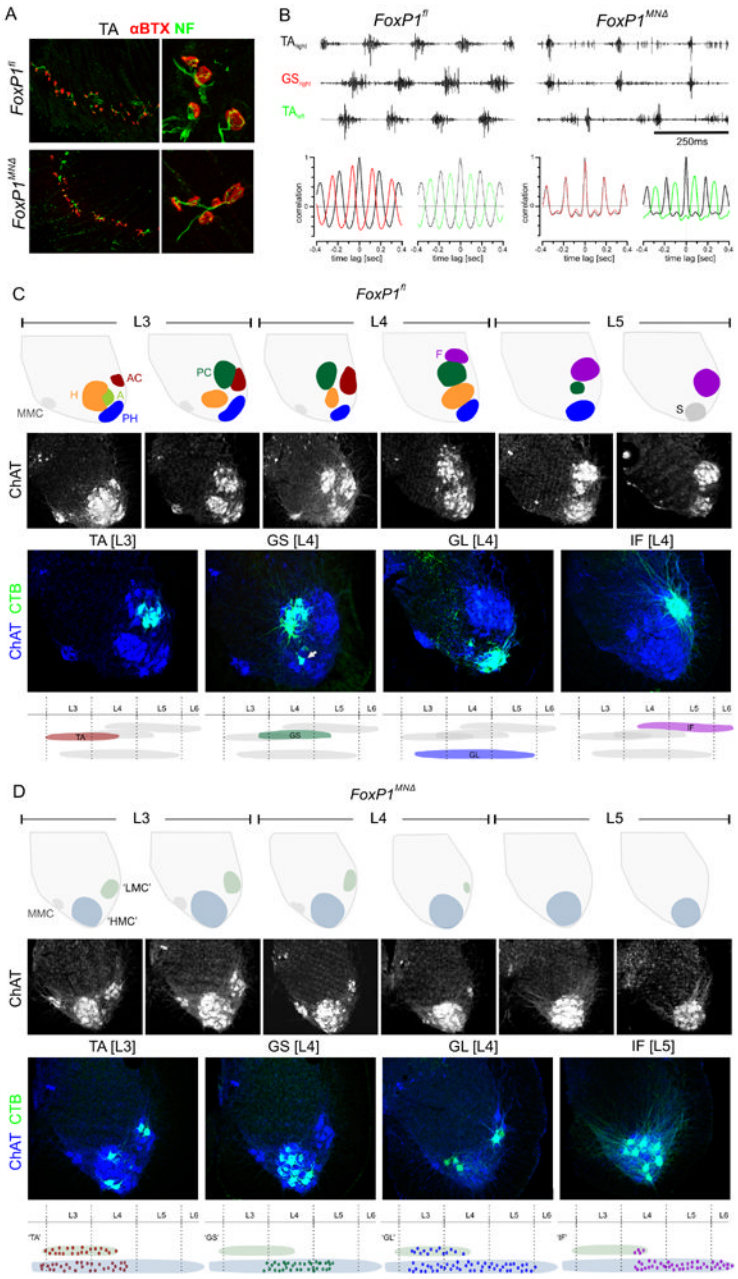

Figure 2. Motor impairment and pool disruption in *FoxP1* mutants

A. Innervation of TA muscle in p2 *FoxP1*^{fl} and *FoxP1*$^{MN\Delta}$ mice. Motor nerves visualized by neurofilament (NF), and acetylcholine receptors by alpha-bungarotoxin (α-BTX) labeling.

B. Upper panels: EMG recodings from right and left TA and right GS muscles from *FoxP1*^{fl} and *FoxP1*$^{MN\Delta}$ mice during swimming. Lower panels: Autocorrelograms of muscle burst patterns of right and left TA and right GS in *FoxP1*^{fl} and *FoxP1*$^{MN\Delta}$ mice.

C. Motor pools in ~p20 *FoxP*^{fl} mice. Top row: columelar positions at L3 to L5, based on our observations and McHanwell and Biscoe (1981). MMC: median motor column, S: sacral motor neurons. Second row: ChAT^{+} motor neurons at L3 to L5. Third row: organization of motor pools after CTB injection into specific muscles. Arrow in GS panel indicates BF and/

NIH-PA Author Manuscript

NIH-PA Author Manuscript

NIH-PA Author Manuscript

or ST motor neurons, labeled through tracer leakage from GS muscle. Bottom row: rostrocaudal distribution of motor pools.

D. Motor neuron position in *FoxP1*$^{MN\Delta}$ mice. Top row: motor neuron positions at L3 to L5. Green/gray: zone 1; blue/gray: zone 2. Second row: ChAT^{+} motor neuron position at L3 to L5. Third row: distribution of motor neuron pools after CTB injection into individual muscles. Bottom row: rostrocaudal distribution of labeled motor neurons. See also Figures S3, S4.

NIH-PA Author Manuscript
NIH-PA Author Manuscript
NIH-PA Author Manuscript

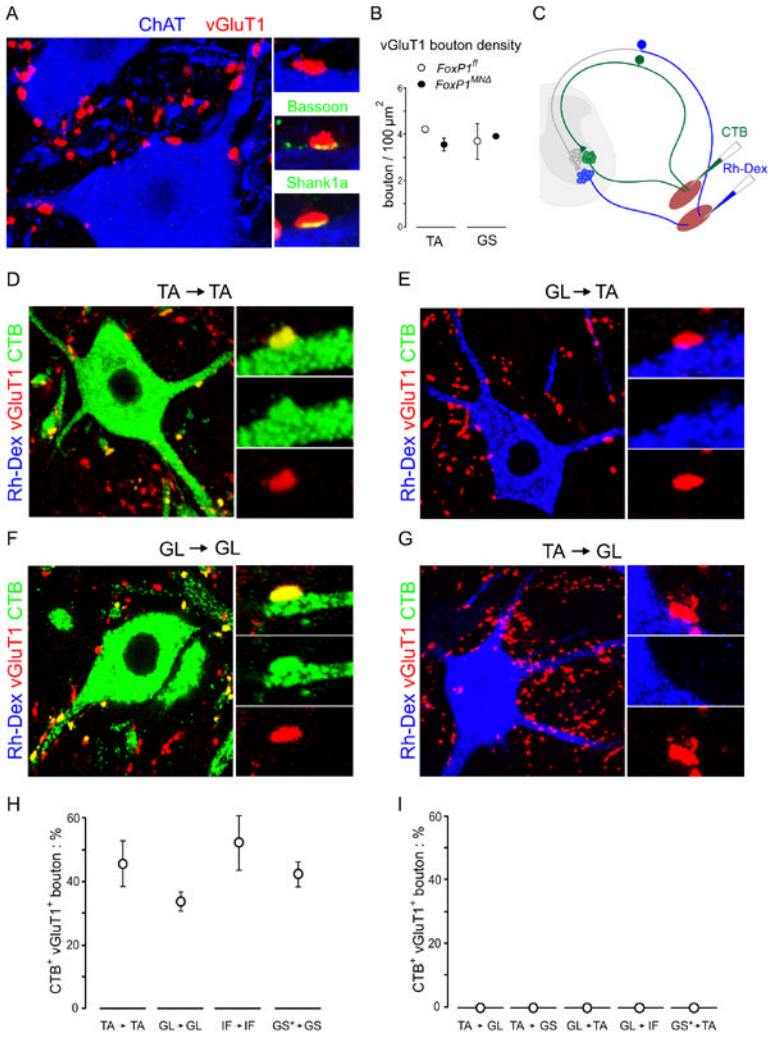

Figure 3. Specifity of sensory connections in wild type mice

A. vGluT1^{+} sensory boutons on ChAT^{+} motor neurons in p18 mice. Bassoon marks sensory terminals and shank1a, motor neuron membrane aligned with sensory boutons.

B. vGluT1^{+} bouton density on TA and GS motor neurons in *FoxP1^{fl}* and *FoxP1$^{MN\Delta}$* mice.

C. Experimental design: after CTB and Rh-Dex tracer injection into different muscles vGluT1^{+} sensory boutons contact CTB-labled ‘self’ but not Rh-Dex-labeled ‘non-self’ motor neurons in p21 wild type mice (See Figure S6).

D. CTB-labeled vGluT1^{+} TA sensory boutons on TA motor neurons.

E. CTB-labeled vGluT1^{+} GL sensory boutons are not found on TA motor neurons.

F. CTB-labeled vGluT1^{+} GL sensory boutons on GL motor neurons.

G. CTB-labeled vGluT1^{+} TA sensory boutons are not detected on GL motor neurons.

H. Incidence of sensory connections with ‘self’ motor neurons. GS* indicates contamination of GS by BF and ST sensory afferents.

I. Incidence of sensory connections with ‘non-self’ motor neurons.

NIH-PA Author Manuscript

NIH-PA Author Manuscript

NIH-PA Author Manuscript

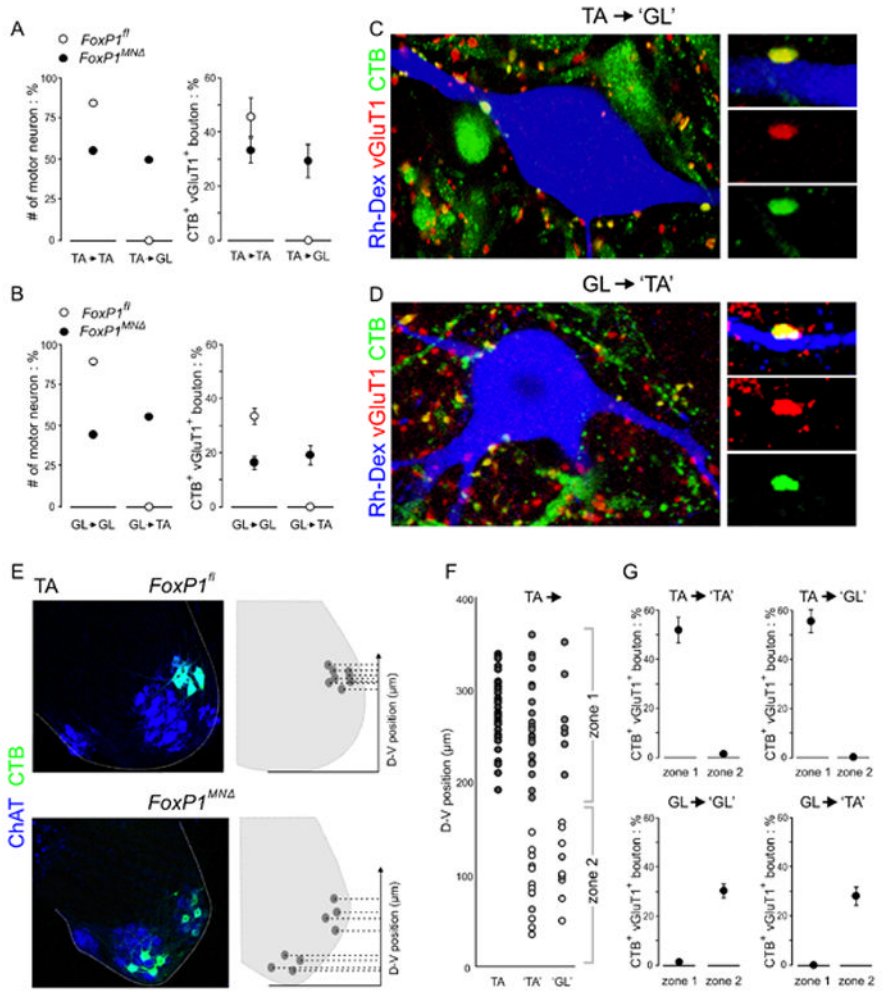

Figure 4. Breakdown of dorsoventral sensory-motor specificity in FoxP1 mutants

A. Incidence of TA sensory input to TA and GL motor neurons in *FoxP1*^{fl} and *FoxP1*$^{MN\Delta}$ mice. Statistical analysis for these and subsequent histograms presented in Figure S7.

B. Incidence of GL sensory input to GL and TA motor neurons in *FoxP1*^{fl} and *FoxP1*$^{MN\Delta}$ mice.

C. CTB-labeled, vGluT1^{+} TA sensory boutons contact 'GL' motor neurons in *FoxP1*$^{MN\Delta}$ mutants.

D. CTB-labeled, vGluT1^{+} GL sensory boutons contact 'TA' motor neurons in *FoxP1*$^{MN\Delta}$ mutants.

E. Plotting the dorsoventral position of CTB-labeled motor neurons (in this case TA and 'TA' neurons) in *FoxP1*^{fl} and *FoxP1*$^{MN\Delta}$ mice.

F. Sensory input status as a function of motor neuron dorsoventral position. Dark grey circles: wild type TA motor neurons. 'TA' and 'GL' motor neurons with CTB-labeled sensory bouton input are shown in light gray circles.'TA' and 'GL' motor neurons lacking CTB-labeled sensory input are shown in open circles.

G. Incidence of sensory input to 'TA' and 'GL' motor neurons in *FoxP1*$^{MN\Delta}$ mutants, gated to zonal position.

See also Figure S7.

NIH-PA Author Manuscript

NIH-PA Author Manuscript

NIH-PA Author Manuscript

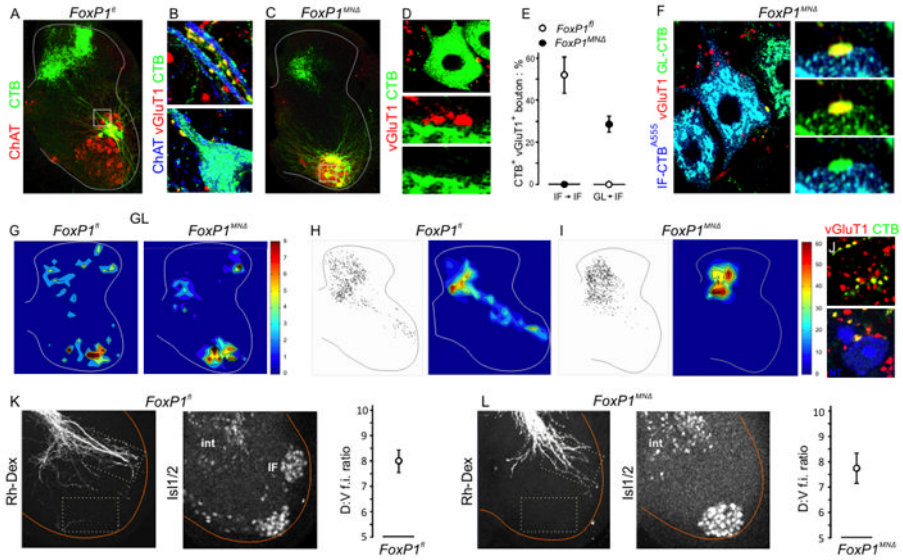

Figure 5. Trajectory of sensory afferents to motor neuron-free domains in *FoxP1$^{MN\Delta}$* mice

A. CTB-labeled IF sensory afferents and ChAT^{+} IF motor neurons in p21 control mice. Position of high power images in B shown as box.

B. CTB-labeled vGluT1^{+} IF sensory boutons on dendrites and cell bodies of IF motor neurons in control mice.

C. CTB-labeled IF sensory afferents and ChAT^{+} IF motor neurons in p21 *FoxP1$^{MN\Delta}$* mice. Position of high power images in D shown as boxes.

D. Absence of CTB-labeled vGlut1^{+} IF sensory boutons on the dendrites or cell bodies of 'IF' motor neurons in p21 *FoxP1$^{MN\Delta}$* mice.

E. Incidence of IF and GL sensory bouton inputs to IF motor neurons in *FoxP1^{fl}* and *FoxP1$^{MN\Delta}$* mice.

F. CTB-labeled vGluT1^{+} GL sensory boutons contact ventrally displaced 'IF' motor neurons.

G. Spatial distribution of CTB-labeled vGluT1^{+} GL sensory boutons in p21 *FoxP1^{fl}* and *FoxP1$^{MN\Delta}$* mice.

H. Spatial distribution of CTB-labeled vGluT1^{+} IF sensory boutons in p21 *FoxP1^{fl}* mice. In H. and I. representative stacks of three (left) and ten (right, color plot) sections are shown.

I. Spatial distribution of CTB-labeled vGluT1^{+} IF sensory boutons in p21 *FoxP1$^{MN\Delta}$* mice.

J. In *FoxP$^{MN\Delta}$* mice, CTB-labeled vGluT1^{+} IF sensory boutons contact neurotrace (NT)-labeled interneurons (blue) in a dorsomedial domain.

K. Left panel: trajectory of sensory afferents at L6 after Rh-Dex labeling of L5 dorsal roots in e18 *FoxP1^{fl}* embryos. Middle panel: Isl1/2^{+} IF motor neurons. Right panel: positional prevalence of Rh-Dex labeled sensory axons. Ratio of mean fluorescence intensity (f.i.) in dorsal and ventral domains determined from 8 sections from 3 mice.

L. Left panel: trajectory of sensory afferents at L6 after Rh-Dex labeling of L5 dorsal roots in e18 in *FoxP1$^{MN\Delta}$* embryos. Middle panel: Isl1/2^{+} IF motor neurons. Right panel: positional prevalence of Rh-Dex labeled sensory axons. Ratio of mean fluorescence intensity (f.i.) in dorsal and ventral domains determined from 8 sections from 3 mice.

NIH-PA Author Manuscript
NIH-PA Author Manuscript
NIH-PA Author Manuscript

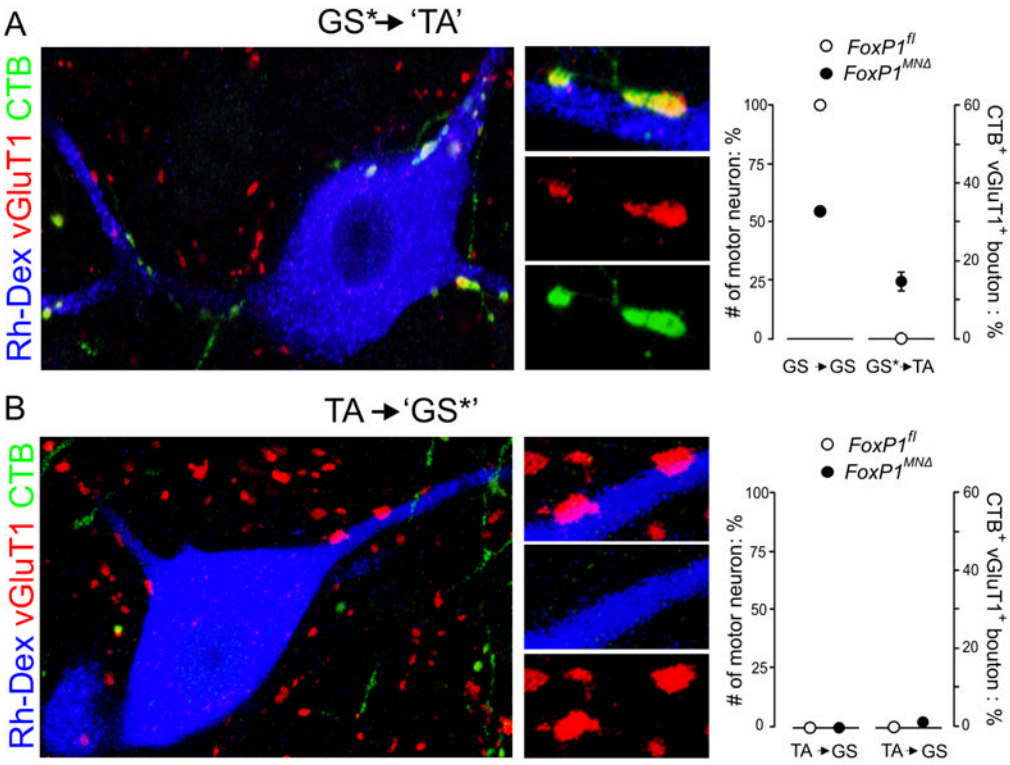

Figure 6. Breakdown of specificity in antagonist reflex arcs in FoxP1 mutants

A. CTB-labeled vGluT1^{+} GS* sensory boutons contact 'TA' motor neurons in p21 *FoxP1*$^{MN\Delta}$ mice. Plots show connectivity of GS* sensory boutons with TA and GS motor neurons in *FoxP1*^{fl} and *FoxP1*$^{MN\Delta}$ mice.

B. CTB-labeled vGluT1^{+} TA sensory boutons contact 'GS*' motor neurons in p21 *FoxP1*$^{MN\Delta}$ mice. Plots show connectivity of TA sensory boutons with TA and GS motor neurons in *FoxP1*^{fl} and *FoxP1*$^{MN\Delta}$ mice.

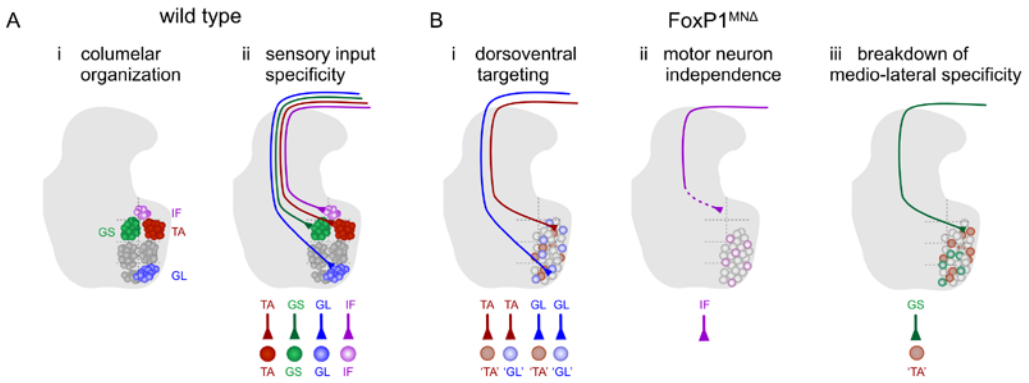

Figure 7. Tier targeting provides a template for sensory-motor connectivity

Ai. Motor columels in wild type mice.

Aii. Tier termination of group Ia sensory afferents supplying individual muscles.

Bi. Tier targeting of TA (red) and GL (blue) sensory afferents in *FoxP1*$^{MN\Delta}$ mice, despite scrambling of 'TA' and 'GL' motor neuron position.

Bii. Tier targeting of sensory afferents at perinatal stages in *FoxP1*$^{MN\Delta}$ mice, despite the absence of tier 1 motor neurons. At later stages, sensory afferents withdraw to a dorsomedial position.

Biii. Breakdown of TA and GS antagonist exclusion in in *FoxP1*$^{MN\Delta}$ mice.

NIH-PA Author Manuscript NIH-PA Author Manuscript NIH-PA Author Manuscript